How Does a Reaction Change Its Mechanism? General Base Catalysis of the Addition of Alcohols to 1-Phenylethyl Carbocations[1]

Rachel Ta-Shma[†] and William P. Jencks*

Contribution No. 1604 from the Graduate Department of Biochemistry, Brandeis University, Waltham, Massachusetts 02254. *Received June 23, 1986*

Abstract: Structure–reactivity correlations are reported for general base catalysis of the addition of alcohols to 1-(4-(dimethylamino)phenyl)ethyl and 1-(4-methoxyphenyl)ethyl carbocations in 50:40:10 H_2O:CF_3CH_2OH:ROH. The addition of trifluoroethanol to the relatively stable ((dimethylamino)phenyl)ethyl cation is catalyzed by substituted acetate ions with $\beta = 0.33$, which is larger than $\beta = 0.23$ for addition to the (methoxyphenyl)ethyl cation. Catalysis is more important for the more stable carbocation, but it decreases faster with increasing alcohol basicity. For the "water catalysis" of alcohol addition to 1-phenylethyl carbocations there is an increased sensitivity to the basicity of ROH with increasing carbocation stability (a "Hammond effect"). This indicates a small involvement of proton transfer in the transition state and is consistent with simple hydrogen bonding of ROH to a base; it is described by a positive interaction coefficient $p_{yy'} = \partial\beta_{nuc}/-\partial\sigma$ (Richard, J. P.; Jencks, W. P. *J. Am. Chem. Soc.* **1984**, *106*, 1396). However, for the acetate-catalyzed reaction there is no significant increase in the sensitivity to ROH basicity with increasing carbocation stability. This represents a decrease in the $p_{yy'}$ coefficient and a shift toward the negative $p_{yy'}$ coefficient that is expected for a fully concerted, coupled mechanism. This change in $p_{yy'}$ and other changes in interaction coefficients describe interrelated changes in the transition state structure that accompany changes in reaction mechanism. They may be described by third derivatives of log k, such as $p^*_{xyy'} = \partial p_{yy'}/-\partial pK_{BH} = \partial p_{xy}/-\partial pK_{nuc} = \partial p_{xy'}/-\partial\sigma$; for these 1-phenylethyl carbocations, $p^*_{xyy'} = 0.011$.

The term "change in reaction mechanism" is often used with two quite different meanings, which it is important to distinguish. First, there may be changes in structure–reactivity coefficients or other properties that describe the *appearance* of the transition state, as in concerted bimolecular substitution reactions that proceed through a carbocation-like transition state. Second, there may be a change from one mechanism to a different mechanism, as in the change from a concerted one-step substitution reaction to a two-step mechanism that proceeds through a carbocation intermediate with a significant lifetime. A change in the appearance of the transition state is not really a change in reaction mechanism; it may or may not be accompanied by a change in the reaction mechanism.

We are concerned here with changes in the properties of reaction mechanisms for general acid–base catalysis of the expulsion and addition of ROH at electrophilic centers. These changes eventually bring about a change from a concerted mechanism of general acid catalysis to a stepwise mechanism of specific acid catalysis of alcohol expulsion. We describe here some interrelated changes in the appearance of the transition state for this reaction that are associated with the change from a concerted to a stepwise mechanism. However, it is not known at exactly what point the proton transfer proceeds in a separate step with a significant barrier.

The addition of an alcohol or water to an electrophilic center requires the removal of a proton before, during, or after the addition step; the reverse reaction involves the corresponding sequence in the opposite direction. It is well-known that proton removal before or during the reaction becomes more significant as ROH becomes more acidic and the electrophilic reagent becomes less reactive.[2-13] General base catalysis occurs when there is significant proton transfer during the addition step; it may involve either a fully concerted coupled mechanism (eq 1) or simple hydrogen bonding to the attacking alcohol that stabilizes the

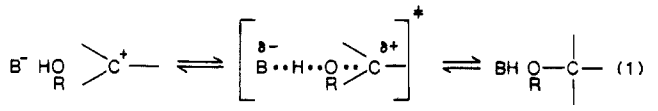

(1)

developing positive charge in the transition state.[2-18] The reverse reaction occurs with general acid catalysis according to the same mechanism. Specific acid catalysis, with proton transfer to the leaving oxygen atom in an initial equilibrium step, occurs with unstable electrophilic reagents and basic alcohols; it corresponds to the uncatalyzed addition of ROH.[10,12,19]

We would like to have a better understanding of the reasons that a particular mechanism is followed and the way in which one mechanism changes to another as the properties of the reactants change. Concerted general acid–base catalysis is characterized by its structure–reactivity coefficients, such as β for general base catalysis, β_{nuc} or β_{lg} for the attacking or leaving alcohol, and ρ for the reactivity of the electrophile. The structure–reactivity behavior can be used to construct an energy contour diagram with a saddle point and reaction coordinate that are defined by the structure–reactivity coefficients for a particular reaction.[20,21]

[†] Present Address: Pre Academic School, Hebrew University, Mount Scopus, Jerusalem, Israel.

(1) This research was supported in part by grants from the National Institutes of Health (GM 20888) and the National Science Foundation (PCM 81-17816).

(2) Fife, T. H. *Acc. Chem. Res.* **1972**, *5*, 264-272.
(3) Gravitz, N.; Jencks, W. P. *J. Am. Chem. Soc.* **1974**, *96*, 507-515.
(4) Capon, B.; Nimmo, K. *J. Chem. Soc., Perkin Trans. 2* **1975**, 1113-1118.
(5) Dunn, B. M. *Int. J. Chem. Kinet.* **1974**, *6*, 143-159.
(6) Bernasconi, C. F.; Gandler, J. R. *J. Am. Chem. Soc.* **1978**, *100*, 8117-8124.
(7) Jensen, J. L.; Herold, L. R.; Lenz, P. A.; Trusty, S.; Sergi, V.; Bell, K.; Rogers, P. *J. Am. Chem. Soc.* **1979**, *101*, 4672-4677.
(8) Gilbert, H. F.; Jencks, W. P. *J. Am. Chem. Soc.* **1982**, *104*, 6769-6779.
(9) Bunton, C. A.; Carrasco, N.; Davoudazadeh, F.; Watts, W. E. *J. Chem. Soc., Perkin Trans. 2* **1980**, 1520-1528. Bunton, C. A. *J. Am. Chem. Soc.* **1981**, *103* 3855-3858.
(10) Jencks, W. P. *Acc. Chem. Res.* **1976**, *9*, 425-432.
(11) Richard, J. P.; Jencks, W. P. *J. Am. Chem. Soc.* **1984**, *106*, 1396-1401.
(12) Jensen, J. L.; Wuhrman, W. B. *J. Org. Chem.* **1983**, *48*, 4686-4691.
(13) Gandler, J. R. *J. Am. Chem. Soc.* **1985**, *107*, 8218-8223.
(14) Sayer, J. M.; Jencks, W. P. *J. Am. Chem. Soc.* **1977**, *99*, 464-474.
(15) Funderburk, L. H.; Aldwin, L.; Jencks, W. P. *J. Am. Chem. Soc.* **1978**, *100*, 5444-5459.
(16) Bergstrom, R. G.; Cashen, M. J.; Chiang, Y.; Kresge, A. *J. Org. Chem.* **1979**, *44*, 1639-1642.
(17) Palmer, J. L.; Jencks, W. P. *J. Am. Chem. Soc.* **1980**, *102*, 6472-6481.
(18) Ritchie, C. D.; Wright, D. J.; Huang, D.-S.; Kamego, A. A. *J. Am. Chem. Soc.* **1975**, *97*, 1163-1170.
(19) Cordes, E. H.; Bull, H. G. *Chem. Rev.* **1974**, *74*, 581-603.

0002-7863/86/1508-8040$01.50/0

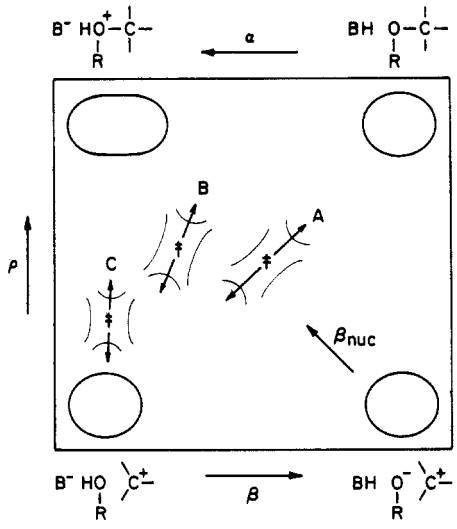

Figure 1. Reaction coordinate energy contour diagram for general base catalysis of the addition of water or alcohols to electrophilic reagents and for the reverse acid-catalyzed reaction. The x and y axes represent proton transfer and C–O bond formation and are defined by β and ρ, respectively. A diagonal axis, y', represents charge development on the alcohol oxygen atom, as measured by β_{nuc}. Reaction coordinates A and B represent general base catalysis (general acid catalysis in the reverse direction) and C represents specific acid-catalyzed cleavage or uncatalyzed addition. Each reaction coordinate passes through a saddle point, but most of the energy contour lines are omitted for clarity.

Changes in structure–reactivity coefficients determine the direction of the reaction coordinate and the curvature of the energy surface parallel and perpendicular to the reaction coordinate.

Figure 1 is a reaction coordinate energy diagram that is defined by the structure–reactivity coefficients β and ρ for the x and y axes and β_{nuc} for a diagonal axis, y', from the lower right to the upper left corner. A change in a structure–reactivity parameter represents movement of the transition state and produces a new diagram with a slightly shifted position of the reaction coordinate.[11,20,21]

General base catalysis of the addition of alcohols and water to aldehydes and other relatively stable electrophiles proceeds through a fully concerted mechanism with a diagonal reaction coordinate on such a diagram, as shown in A of Figure 1.[15,17,20] The observed structure–reactivity coefficients and the position of the transition state on the energy diagram change in a predictable way with changing structure of the reactants for such a mechanism. For this reaction they give a negative value for the cross-interaction coefficient $p_{yy'}$ (eq 2). This corresponds to reaction coordinate A, with a large diagonal component. The $p_{yy'}$ coefficient describes the relationship between the amount of charge development on the oxygen atom of the alcohol in the transition state, as measured by the dependence of log k on pK_{nuc} (β_{nuc}) and

$$p_{yy'} = \partial\beta_{nuc}/-\partial\sigma = \partial\rho/-\partial pK_{nuc} \qquad (2)$$

the stability of the carbocation, which decreases with increasing σ. The negative values of $p_{yy'}$ are based on changes in α-secondary deuterium isotope effects for the addition of alcohols to formaldehyde with changing pK_{ROH}[17] and ratios of the rate constants for general base catalysis of alcohol addition to formaldehyde and acetaldehyde that decrease with decreasing pK_{ROH},[22] which corresponds to a negative $\partial\rho/-\partial pK_{nuc}$. Other structure–reactivity correlations provide additional evidence for the concerted reaction mechanism.[15]

Less stable electrophilic reagents, such as substituted 1-phenylethyl carbocations, show structure–reactivity behavior that suggests a change to a mechanism with less proton transfer from the attacking alcohol.[11] This mechanism appears to involve simple hydrogen bonding between the attacking alcohol and the base catalyst in the transition state and does not require fully concerted proton transfer. The reaction coordinate that is defined by the structure–reactivity behavior of the water-catalyzed reaction is largely vertical on the energy diagram, as shown by B in Figure 1. This reaction coordinate involves primarily bond formation and cleavage at carbon, along the y coordinate, with relatively little motion of the proton, along the x coordinate.

This conclusion is based on the observed increase in β_{nuc}, which reflects the amount of bond formation to the nucleophile in the transition state, as the carbocation becomes less reactive (decreased σ). It represents a normal "Hammond effect" and is defined by a positive value of the cross-interaction coefficient $p_{yy'}$ (eq 2).[11,20] A positive value of $p_{yy'}$ corresponds to a largely vertical reaction coordinate with hydrogen bonding to the base in the transition state, B in Figure 1. A horizontal cross section across the diagram through the saddle point corresponds to an energy well for motion of the proton in the transition state of this reaction.

When the electrophilic reagent becomes still less stable and the alcohol is basic, general acid–base catalysis disappears and the reaction proceeds through a stepwise mechanism of uncatalyzed addition, which is specific acid-catalyzed cleavage in the reverse direction. This is shown by reaction coordinate C in Figure 1. The best known example is specific acid catalysis of the cleavage of sucrose and other acetals.[19] The positive deviation of the rate constant for uncatalyzed water addition to triarylmethyl cations from the Brønsted plot for general base catalysis of water addition suggests that this mechanism may occur concurrently with the concerted mechanism.[13]

Grunwald has shown that concerted general base catalysis of the addition of alcohols to formaldehyde can also be described satisfactorily by a simple energy contour diagram that assumes a reaction coordinate with an angle of 45°.[23] However, such a diagram does not take into account the possibility of changes in the contribution of the proton-transfer process in the transition state that are described by changes in the direction of the reaction coordinate, such as A and B in Figure 1.

The experiments described here were carried out in order to extend the range of reactivity for general base catalysis of the addition of ROH to carbocations with the goal of examining the transition region between the predominantly vertical reaction coordinate for the addition of water to unstable carbocations and the diagonal reaction coordinate for addition to more stable electrophiles, such as carbonyl compounds. We have found that there is little or no change in β_{nuc} with increasing stability of the carbocation for general base catalysis by acetate ion of the addition of alcohols to 1-(4-(dimethylamino)phenyl)ethyl and 1-(4-methoxyphenyl)ethyl carbocations (**1**), Me_2N–R^+ and MeO–R^+. This shows that there is a decrease in the value of $p_{yy'}$ and a more diagonal reaction coordinate for catalysis by acetate compared with water. It confirms the conclusion that these reactions are in the "borderline" region in which the mechanism of catalysis is changing, although there is no evidence for discontinuity or nonlinearity in the structure–reactivity correlations.

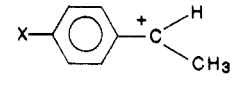

1a: X = Me_2N
1b: X = MeO

Experimental Section

Materials. Commercial reagents were analytical grade or Aldrich Gold Label compounds when available. Dichloroacetic acid, methoxyacetic acid, dichloroethanol, chloroethanol, cyanoethanol, and methyl mercaptoacetate were redistilled. Thiols were stored under nitrogen or argon. Trifluoroethanol (Aldrich, Gold Label) was used only if an aqueous solution showed a pH above 5, and the material was shown to be pure by HPLC. Water was glass distilled. 1-(4-(Dimethylamino)-phenyl)ethyl alcohol and 1-(4-methoxyphenyl)ethyl 4-nitrobenzoate were prepared as described previously.[24] The methyl and ethyl ethers of

(20) Jencks, D. A.; Jencks, W. P. *J. Am. Chem. Soc.* **1977**, *99*, 7948–7960.
(21) Jencks, W. P. *Chem. Rev.* **1985**, *85*, 511–527.
(22) Sørensen, P. E.; Jencks, W. P., in preparation.
(23) Grunwald, E. *J. Am. Chem. Soc.* **1985**, *107*, 4710–4715.

1-(4-(dimethylamino)phenyl)ethyl alcohol were prepared by reaction of 2.4×10^{-5} M alcohol in methanol or ethanol containing 8×10^{-5} M hydrochloric acid at 45 °C. The reaction was followed by HPLC and was complete after 1–2 h. The acid was neutralized with equimolar sodium bicarbonate. The solution was concentrated by rotary evaporation and stored at −15 °C; it contained <0.5% impurities by HPLC analysis.

Procedures. Solvolysis reactions were carried out in a solvent consisting of equal volumes of an aqueous solution containing buffer, maintained at ionic strength 1.0 with potassium nitrate, and of trifluoroethanol or a mixture of trifluoroethanol and another alcohol. The solvolysis of 1-(4-(dimethylamino)phenyl)methyl ether and ethyl ether was carried out in the presence of acetate buffer or dilute hydrochloric acid to give apparent pH values in the range 4.8–5.7. The pK_a of the N-protonated substrate is 5.5, and only the acid-catalyzed cleavage of the free base is significant under the conditions of these experiments.[25] Reactions were initiated by forcefully injecting 0.2–0.4 mL of the solvolysis solution into a round-bottomed test tube containing 2–4 μL of concentrated ether in methanol to give a final substrate concentration in the range 2–5 mM. After 30–60 s at room temperature (22 ± 2 °C) 2–6% reaction had occurred and the sample was quenched by rapid injection of an aliquot into half its volume of 1 M potassium carbonate containing 0.022 M methyl mercaptoacetate, to give a final pH of >9.1. For runs containing no acetate, aliquots were quenched with an equal volume of 1 M potassium bicarbonate to give a final pH of >8.8. Quenching decreases the solvolysis rate by a factor of $\geq 10^3$. The samples were kept at −15 °C until they were analyzed by HPLC.

Methyl mercaptoacetate was added in order to trap any carbocation that was formed from an acetate ester of the substrate under the alkaline conditions of the quenching solution. The carbocation that is formed in the solvolysis mixtures reacts with the basic component of buffers to give the ester as a transient intermediate, which itself reacts rapidly to regenerate the carbocation. Approximately 50 and 6% of the initial product after 60 s is ester with 0.5 M acetate and chloroacetate anions, respectively. If methyl mercaptoacetate is not present in the quench solution the carbocation, regenerated from the acetate ester in the alkaline quench solution, will react exclusively with trifluoroethanol anion ($k_{TFE^-}/k_{HOH} = 2.2 \times 10^5$).[24] This will increase the reaction product ratio [Me_2N–R–OTFE]/[Me_2N–R–OH].

Product ratios from the solvolysis of 1-(4-methoxyphenyl)ethyl 4-nitrobenzoate in water–alcohol mixtures were determined as described previously.[11,24]

Product ratios were measured by HPLC with a Waters Associates reverse phase octadecylsilane column (Nova Pack C_{18} 5μ) as described previously.[24] The formation of 1-(4-(dimethylamino)phenyl)ethyl methoxyethyl ether was determined with the ethyl rather than the methyl ether as substrate because this product coelutes with the methyl ether. The acetate-catalyzed reaction of trifluoroethanol in the presence of 10% ethanol was not examined because 1-(4-(dimethylamino)phenyl)ethyl ether coelutes with the methyl mercaptoacetate derivative, so that the reaction could not be quenched in the presence of methyl mercaptoacetate.

Ratios of the second-order rate constants for partitioning of the arylethyl cations were calculated from ratios of the reaction products and nucleophile concentrations, from the average value of 3–10 HPLC analyses that usually agreed by better than ±2% for the 1-(4-methoxyphenyl)ethyl carbocation and ±6% for the 1-(4-(dimethylamino)-phenyl)ethyl carbocation. The larger scatter with the latter reaction arises from the fact that only the first 2–6% of the reaction was followed, in order to obtain initial product ratios and avoid secondary reactions of the products.

Results

Catalysis of the addition of alcohols to the Me_2N–R^+ and MeO–R^+ carbocations (eq 1) was measured by product analysis after solvolysis of derivatives of Me_2N–R^+ and MeO–R^+ in the presence of increasing concentrations of base catalysts at ionic strength 0.5, maintained with potassium nitrate in H_2O:TFE:ROH, 50:40:10 (v:v:v). Ratios of rate constants for the addition of alcohols, ROH, and water were obtained by HPLC analysis of the products, as shown in eq 3 for reactions of Me_2N–R^+. In eq 3, k^0_{ROH} and k^B_{ROH} are the second- and third-order rate constants for the "uncatalyzed" (or water-catalyzed) and the base-catalyzed reactions of alcohol with the carbocation. Values

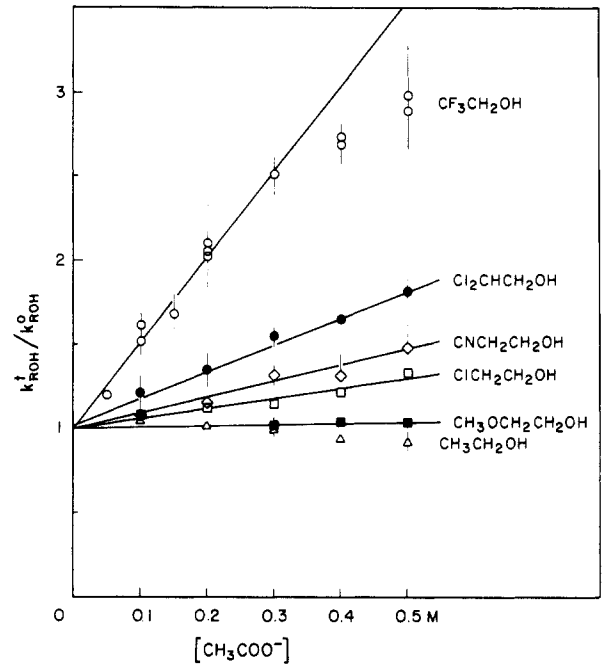

Figure 2. General base catalysis by acetate anion of the reactions of substituted ethanols with 1-(4-(dimethylamino)phenyl)ethyl carbocation in 50:40:10 H_2O:TFE:ROH (v:v:v) at 22 ± 2 °C and ionic strength 0.5, maintained with KNO_3.

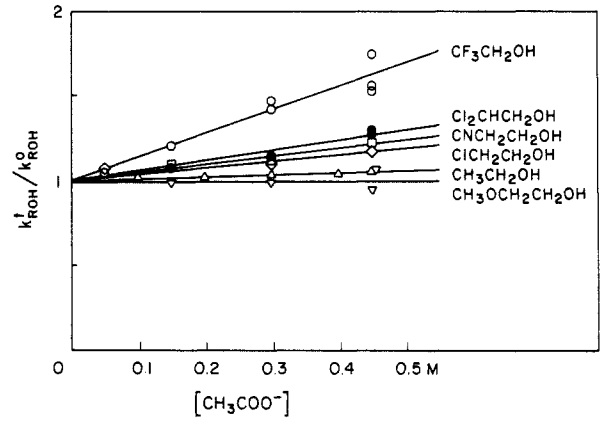

Figure 3. General base catalysis by acetate anion of the reactions of substituted ethanols with 1-(4-methoxyphenyl)ethyl carbocation in 50:40:10 H_2O:TFE:ROH (v:v:v) at 22 ± 2 °C and ionic strength 0.5, maintained with KNO_3.

of k^t_{ROH}/k^0_{ROH} were calculated from observed values of k^0_{ROH}/k_{HOH} in the absence of buffer and k^t_{ROH}/k_{HOH} at each buffer concentration, assuming a constant value of k_{HOH}. The increases in k^t_{ROH}/k^0_{ROH} with increasing concentration of acetate ion for the reactions of alcohols with the Me_2N–R^+ and MeO–R^+ carbocations are shown in Figures 2 and 3, respectively. The increase in reactivity of the alcohols is approximately linear, up to a twofold increase, and becomes larger as the alcohols become more acidic.

$$\frac{k^t_{ROH}}{k_{HOH}} = \frac{[Me_2NPhEtOR][HOH]}{[Me_2NPhEtOH][ROH]} = \frac{k^0_{ROH}}{k_{HOH}} + \frac{k^B_{ROH}[B]}{k_{HOH}} \quad (3)$$

The rate constant for addition of water, k_{HOH}, was used as a reference for estimating catalytic constants for the addition of alcohols because there is no significant change in the ratios k_{HOH}/k_{RSH} and k_{HOH}/k_{az} with increasing acetate concentrations for reactions of MeO–R^+, after correction of the rate constant for the diffusion-controlled reaction of azide,[24] k_{az}, for the change in the viscosity of the solvent (Table I). There is also no significant change in the ratio k_{HOH}/k_{RSH} for reactions of the Me_2N–R^+ carbocation in the presence of increasing concentrations of acetate, although there is a large increase in k^t_{TFE}/k_{RSH} (Table I). The

(24) Richard, J. P.; Rothenberg, M. E.; Jencks, W. P. *J. Am. Chem. Soc.* **1984**, *106*, 1361–1372.
(25) Richard, J. P.; Jencks, W. P. *J. Am. Chem. Soc.* **1984**, *106*, 1373–1383.

Table I. The Effect of Acetate Anion on the Partitioning of 1-Phenylethyl Carbocations in 50:50 TFE:H_2O (v:v) Containing *n*-Propanethiol

1-(4-Methoxyphenyl)ethyl Carbocation[a]

$[CH_3COO^-]$, M	$10^4k_{HOH}/k_{az}$[b]	k_{PrSH}/k_{az}[b]	k_{PrSH}/k_{az} corrected[c]	$10^4k^t_{TFE}/k_{PrSH}$[b]	$10^3k_{HOH}/k_{PrSH}$[b]	$10^3k_{HOH}/k_{az}$ corrected[c]
0	3.76	0.30	0.30	6.7	1.26	0.38
0.15	3.83	0.31	0.29	7.9	1.24	0.37
0.30	4.29	0.33	0.30	9.5	1.29	0.39
0.45	4.51	0.35	0.30	11.2	1.29	0.39

1-(4-(Dimethylamino)phenyl)ethyl Carbocation[d]

$[CH_3COO^-]$, M	$10^5k_{HOH}/k_{PrSH}$[e]	$10^5k^t_{TFE}/k_{PrSH}$[e]
0	9.3	3.4
0.05	9.5	3.9
0.50	9.6	9.4

[a] The 1-(4-methoxyphenyl)ethyl carbocation was generated by the solvolysis of its *p*-nitrobenzoate at 22 ± 2 °C and μ = 0.5, maintained with KNO_3, $[NaN_3]$ = 0.010 M and $[C_3H_7SH] = 2.6 \times 10^{-2}$ M, pH 6.5 (Ac^-/HAc = 20). At this pH the amount of thiolate formed (<0.4%) and its possible contribution to the thiol product formation are negligible, $pK_{C_3H_7SH}$ = 10.5 in water (Hupe, D. J.; Jencks, W. P. *J. Am. Chem. Soc.* **1977**, *99*, 451), and k_{RS^-}/k_{RSH} = 3.3.[24] [b] Dimensionless ratio of second-order rate constants, from the average of 4–6 injections to the HPLC column that agreed to ±2%. [c] Corrected for the effect of viscosity on k_{az}, from the measured 19% increase in viscosity upon substituting 0.5 M CH_3COONa for 0.5 M KNO_3 in 50:50 (v:v) H_2O:TFE, assuming that the change in k_{az} is proportional to the change in the viscosity and that the viscosity increases linearly up to 0.5 M $[CH_3COONa]$. [d] The 1-(4-(dimethylamino)phenyl)ethyl carbocation was generated by acid catalysis from its methyl ether at 22 ± 2 °C and pH 5.12 (acetate buffer 1:1), μ = 0.5, maintained with KNO_3. Azide does not give a stable product with this cation.[24] $[C_3H_7SH] = (2.2\text{–}2.7) \times 10^{-3}$ M. [e] Dimensionless ratio of second-order rate constants, from the average of 3 injections to the HPLC column that agreed to ±6%.

Table II. The Effect of Acetate Anion on the Partitioning of 1-Phenylethyl Carbocations in 50:40:10 (v:v:v) H_2O:TFE:Cl_2CHCH_2OH, Ionic Strength 0.5 (KNO_3)

1-(4-methoxyphenyl)ethyl carbocation			1-(4-(dimethylamino)phenyl)ethyl carbocation		
$[CH_3COO^-]$, M	k^t_{TFE}/k_{HOH}	$k^t_{Cl_2CHCH_2OH}/k_{HOH}$	$[CH_3COO^-]$, M	k^t_{TFE}/k_{HOH}	$k^t_{Cl_2CHCH_2OH}/k_{HOH}$
0	0.49	1.94	0	0.38[a]	1.52[a]
0.15	0.60	2.05	0.1	0.55	1.85
0.30	0.69	2.19	0.2	0.76	2.05
0.45	0.82[a]	2.47[a]	0.3	0.90	2.35
0.90[b]	1.09	3.12	0.4	1.07	2.51
			0.5	1.15	2.76

[a] Average of two experiments; the results differed by less than 5%. [b] At μ = 0.95. The product ratios confirm the general trend but show deviations from the line correlating the data at lower acetate concentrations and ionic strength.

addition or expulsion of thiols is known to show little or no general acid–base catalysis.[26] An increase in viscosity of 20 ± 1% was observed upon substituting 0.5 M sodium acetate for 0.5 M potassium nitrate in 50:50 (v:v) H_2O:TFE, 50:40:10 (v:v:v) H_2O:TFE:EtOH, and 50:40:10 (v:v:v) H_2O:TFE:$CH_3CH_2CH_2OH$.

It is probable that small increases of 27% and 19% in k_{HOH}/k_{az} and k_{MeOH}/k_{az} for MeO–R^+ upon substitution of 0.5 M sodium methoxyacetate for sodium perchlorate are also caused by an effect of viscosity on k_{az}[11] and that the previously reported catalytic constants, which were obtained from uncorrected values of k_{ROH}/k_{az}, are too large for the same reason. If there is no significant catalysis of water addition to Me_2N–R^+ there is certainly no catalysis of water addition to MeO–R^+, which shows considerably less catalysis of ROH addition than Me_2N–R^+. Accordingly, the earlier data[11] were replotted relative to the water reaction, as in eq 3, to give values of k_B for catalysis of trifluoroethanol addition to MeO–R^+ of $10^{-6}k_B/(M^{-2}\ s^{-1})$ = 0.96 for CH_3COO^-, 0.60 for $HCOO^-$, 0.57 for $CH_3OCH_2COO^-$, and 0.036 for H_2O. Catalysis by $CHCl_2COO^-$ and CF_3COO^- is too small to give reliable catalytic constants, but the data are consistent with the Brønsted correlation that is described below. The selectivity of k_{RSH}/k_{TFE} = 1500 for the reaction of propanethiol with MeO–R^+ (Table I) is close to a previously reported value for this ratio of 1700 under the same conditions, except that the ionic strength was maintained at 0.5 with sodium perchlorate.[25] The larger value of k_{RSH}/k_{TFE} = 29400 for Me_2N–R^+ (Table I) represents a normal "Hammond effect".

Table II shows typical data for catalysis by acetate ion of the addition of trifluoroethanol and dichloroethanol to the MeO–R^+ and Me_2N–R^+ carbocations. The less reactive Me_2N–R^+ cation shows a slightly larger selectivity for water over trifluoroethanol than the MeO–R^+ cation in the absence of catalyst, but the more effective catalysis of the addition of trifluoroethanol to Me_2N–R^+ results in a reversal of this ratio as the concentration of the base catalyst is increased. The slopes and intercepts of the plots of

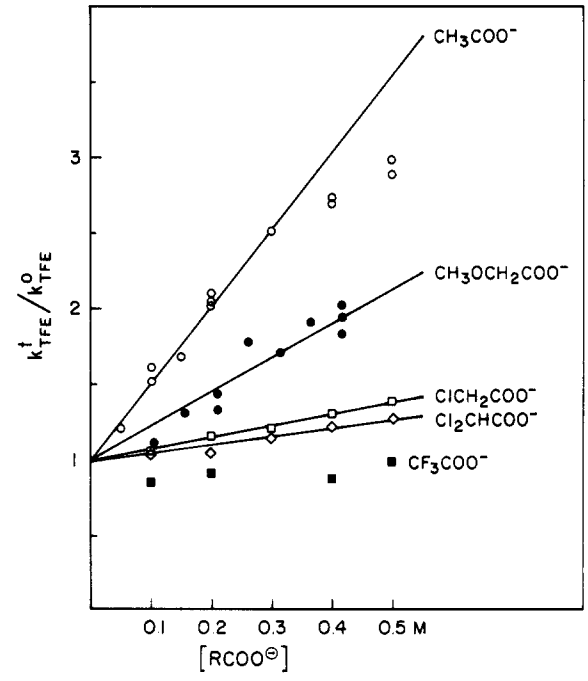

Figure 4. General base catalysis by carboxylate anions of the reaction between trifluoroethanol and 1-(4-(dimethylamino)phenyl)ethyl cation in 50:50 (v:v) H_2O:TFE at ionic strength 0.5, maintained with KNO_3.

Table III. Rate Constants for the Acetate-Catalyzed and Uncatalyzed Reactions of Alcohols with the 1-(4-(Dimethylamino)phenyl)ethyl Carbocation and the 1-(4-Methoxyphenyl)ethyl Carbocation

	4-$CH_3OC_6H_4CHCH_3^+$ [a]				4-$(CH_3)_2NC_6H_4CHCH_3^+$ [b]		
ROH	pK_N [c]	k^0_{ROH}/k_{HOH} [d]	k^B_{ROH}/k_{HOH} [e], M^{-1}	k^B_{ROH}/k^0_{ROH}, M^{-1}	k^0_{ROH}/k_{HOH} [d]	k^B_{ROH}/k_{HOH} [e], M^{-1}	k^B_{ROH}/k^0_{ROH}, M^{-1}
CF_3CH_2OH	5.81 [f]	0.49	0.68	1.4	0.33	1.7	5.1
Cl_2CHCH_2OH	7.14 [g]	1.9	1.15	0.60	1.5	2.4	1.6
$CNCH_2CH_2OH$	8.03 [f]	1.8	0.88	0.48	1.7	1.63	0.95
$ClCH_2CH_2OH$	8.81 [f]	4.0	1.5	0.375	4.5	2.7	0.60
$CH_3OCH_2CH_2OH$ [h]	9.72 [i]	5.8	≤1.4 [j]	<0.24	8.5	≤1.5 [j]	≤0.2
CH_3CH_2OH	10.97 [i]	11.7	<2.1 [j]	<0.19 [j]	27	≤0 [k]	

[a] Generated from 1-(4-methoxyphenyl)ethyl 4-nitrobenzoate in 50:40:10 (v:v:v) H_2O:TFE:ROH containing 0.010 M NaN_3 at 22 ± 2 °C, pH 7.6–7.9 (no buffer). Ionic strength 0.50 was maintained with KNO_3. Four to six acetate concentrations in the range 0–0.45 M were used with each alcohol. [b] Generated from 1-(4-(dimethylamino)phenyl)ethyl methyl ether in 50:40:10 (v:v:v) H_2O:TFE:ROH (with EtOH the ratios were 50:45:5 (v:v:v) H_2O:TFE:EtOH) at 22 ± 2 °C and pH 5.1 ([AcO^-][HAc] = 1:1). Ionic strength 0.5 was maintained with KNO_3. Six acetate concentrations in the range 0–0.5 M were used with each alcohol. [c] $pK_N \equiv pK_{BH^+}$ values for the corresponding ethylamines.[25] [d] Dimensionless ratio of second-order rate constants. [e] Calculated from the increase in substituted ethyl ether formation with increasing acetate concentration. [f] At ionic strength 1.0 (Cox, M. M.; Jencks, W. P. *J. Am. Chem. Soc.* **1981**, *103*, 572). [g] Calculated by using the equation $pK_a(RCH_2NH_3^+) = pK_a(CH_3CH_2NH_2^+) - 0.28 - 1.83\sigma^*$ and $\sigma^*_{CHCl_2} = 1.94$ from the following: Perrin, D. D.; Dempsey, B.; Serjeant, E. P. *pK_a Prediction for Organic Acids and Bases*; Chapman and Hall: New York, 1981; pp 39 and 133. [h] The 1-(4-(dimethylamino)phenyl)ethyl carbocation was generated from its ethyl ether. [i] At ionic strength 1.0 (Jencks, W. P.; Gilchrist, M. *J. Am. Chem. Soc.* **1968**, *90*, 2622). [j] The k_{ROH}/k_{HOH} values showed no significant increase. The limit was calculated from the slope consistent with the scatter of the points. [k] The k_{ROH}/k_{HOH} values showed appreciable scatter and a slight tendency to decrease when [AcO^-] increases.

Table IV. Rate Constants for General Base Catalysis of the Reaction of Trifluoroethanol with the 1-(4-(Dimethylamino)phenyl)ethyl Carbocation[a]

base	pK_a [b]	k^B_{TFE}/k_{HOH}, M^{-1}	k^B_{TFE}, M^{-2} s^{-1}
CH_3COO^- [c]	4.6	1.71	111
$CH_3OCH_2COO^-$ [d]	3.33	0.72	47
$ClCH_2COO^-$ [e]	2.65	0.255	17
Cl_2CHCOO^- [f]	1.03	0.167	11
CF_3COO^- [g]	0.23	<0.08	<5.2
H_2O	−1.74		0.79 [h]

[a] Generated from the methyl ether in 50:50 (v:v) H_2O:TFE at 22 ± 2 °C and ionic strength 0.5 maintained with KNO_3. [b] In water, ionic strength 1.0 (Cox, M. M.; Jencks, W. P. *J. Am. Chem. Soc.* **1981**, *103*, 574); the pK_a for CF_3COOH (at lower ionic strength) is from: *Handbook of Biochemistry and Molecular Biology*, 3rd ed.; Gerald D. Fasman, Ed.; CRC Press: Cleveland, 1975; Vol. I, p 309. [c] In [CH_3COO^-]/[CH_3COOH] = 1:1, pH 5.12. [d] In [$CH_3OCH_2COO^-$]/[CH_3OCH_2COOH] = 1:1, pH 4.12. [e] In [$ClCH_2COO^-$]/[$ClCH_2COOH$] = 2:1, pH 3.60. [f] pH 4.8–5.7 with $Cl_2CHCOOH$. [g] pH 3.0–3.1 with HCl. [h] $k^0_{TFE}/[H_2O]$.

experimental data for a larger series of alcohols according to eq 3 are reported in Table III.

Figure 4 shows that catalysis by substituted acetate anions of the addition of trifluoroethanol to Me_2N–R^+ increases with increasing basicity of the catalyst; there is no significant catalysis by trifluoroacetate ion. Values of k^B_{TFE}/k_{HOH} for catalysis by the substituted acetates and absolute values of the catalytic constants, from an estimated value[24] of $k_{HOH} = 65$ M^{-1} s^{-1}, are given in Table IV.

Replacement of trifluoroethanol by less acidic alcohols in the solvent causes a decrease in the reactivity of trifluoroethanol relative to water, as shown in Tables V and VI. This arises from an increase in the rate constant for the reaction of water with MeO–R^+, which is larger than a small increase in the reactivity of trifluoroethanol, as shown by the k_{HOH}/k_{az} and k_{TFE}/k_{az} ratios in Table V. The reaction of azide ion with MeO–R^+ is diffusion controlled,[24] and only a small change in viscosity was observed upon replacing 20% of the trifluoroethanol by ethanol (+1%) or methoxyethanol (+6%). However, k^0_{TFE}/k_{HOH} and k^B_{TFE}/k_{HOH} values show a similar solvent sensitivity, so that there is relatively little change in k^B_{TFE}/k^0_{TFE} with changing ROH in the solvent (Table VI).

These solvent effects may be attributed to inhibition of the reaction of water and alcohols by trifluoroethanol because of the

Table V. Rate Constants for the Uncatalyzed Reaction of 1-(4-Methoxyphenyl)ethyl Carbocation with Trifluoroethanol in the Presence of Other Alcohols[a]

	ROH = $CH_3OCH_2CH_2OH$			ROH = $CNCH_2CH_2OH$		
% ROH	$10^4k_{HOH}/k_{az}$	$10^4k^0_{TFE}/k_{az}$	k^0_{TFE}/k_{HOH}	$10^4k_{HOH}/k_{az}$	$10^4k^0_{TFE}/k_{az}$	k^0_{TFE}/k_{HOH}
0	3.6	1.71	0.48	3.5	1.86	0.54
5	4.6	2.01	0.44	5.0	2.03	0.41
10	6.5	2.47	0.38	6.1	2.08	0.34
20	10.1	2.87	0.28			

[a] At 22 ± 2 °C and $\mu = 0.5$, maintained with KNO_3. The solvolysis mixture consisted of 50% H_2O, (50 − x)% TFE, X% ROH (v:v:v) and [NaN_3] = 0.010 M.

Table VI. Rate Constants for Acetate-Catalyzed and Uncatalyzed Reactions of Trifluoroethanol with 1-(4-Methoxyphenyl)ethyl and 1-(4-(Dimethylamino)phenyl)ethyl Carbocations in 50:40:10 (v:v:v) H_2O:TFE:ROH

	4-$CH_3OC_6H_4CHCH_3^+$ [a]			4-$(CH_3)_2NC_6H_4CHCH_3^+$ [b]		
ROH	k^0_{TFE}/k_{HOH} [c]	k^B_{TFE}/k_{HOH} [d], M^{-1}	k^B_{TFE}/k^0_{TFE}, M^{-1}	k^0_{TFE}/k_{HOH} [c]	k^B_{TFE}/k_{HOH} [d], M^{-1}	k^B_{TFE}/k^0_{TFE}, M^{-1}
CF_3CH_2OH	0.49	0.68	1.4	0.33	1.7	5.1
Cl_2CHCH_2OH	0.50	0.66	1.3	0.38	1.7	4.5
$CNCH_2CH_2OH$	0.34	0.58	1.7	0.23	1.1	4.8
$ClCH_2CH_2OH$	0.44	0.61	1.4	0.23	1.2	5.2
$CH_3OCH_2CH_2OH$	0.40	0.47	1.2	0.20	1.16	5.7
CH_3CH_2OH	0.43	0.68	1.6	0.27 [e]	*f*	

[a] Generated as described in Table III, note *a*. [b] Generated as described in Table III, note *b*. [c] Dimensionless ratio of second-order rate constants. [d] Calculated from the increase in trifluoroethyl ether formation with increasing acetate concentration. [e] In 50:45:5 (v:v:v) H_2O:TFE:EtOH. [f] Not determined (see Experimental Section).

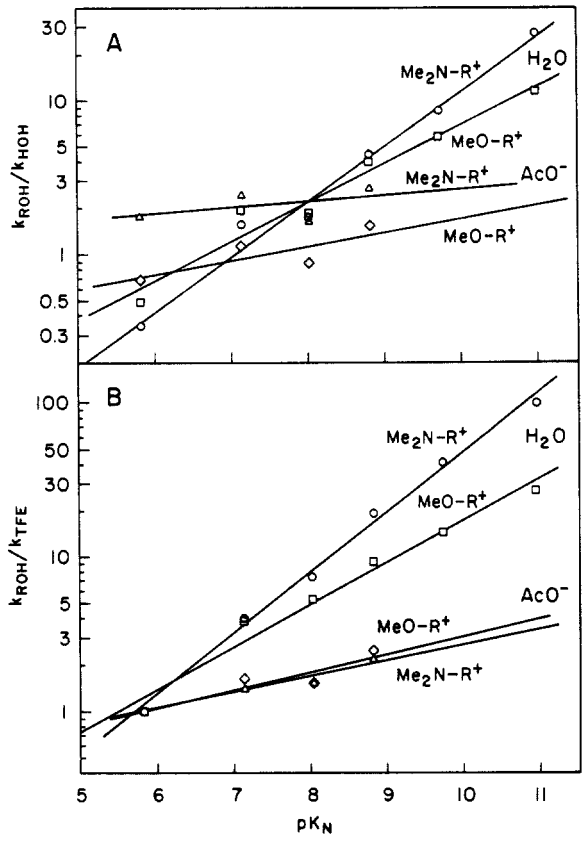

Figure 5. Logarithmic plots of rate constant ratios for the acetate-catalyzed (△ and ◇) and the "water-catalyzed" (○ and □) reactions of substituted ethanols with two 1-arylethyl carbocations. The pK_N values on the abcissa are pK_{BH^+} values for the corresponding substituted ethylamines (see text). A: Values on the ordinate are k^0_{ROH}/k_{HOH} and k^B_{ROH}/k_{HOH} ratios (Table III). B: Values on the ordinate are k^0_{ROH}/k^0_{TFE} and k^B_{ROH}/k^B_{TFE} ratios, calculated from the corresponding values of k_{ROH}/k_{HOH} and k_{TFE}/k_{HOH} (Tables III and IV).

strong hydrogen bonding of trifluoroethanol to the lone-pair electrons of the nucleophile, **2**, and the poor hydrogen bond ac-

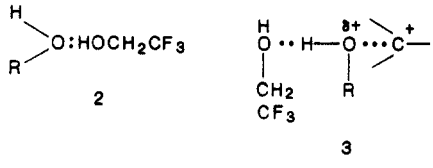

2

3

cepting ability of trifluoroethanol in the transition state, **3**.[24-27] Inhibition by hydrogen bonding to the lone-pair electrons, **2**, might be expected to be more important for the relatively basic water molecule than for trifluoroethanol.

On the other hand, replacement of trifluoroethanol by *water* in the solvent mixture has the opposite effect; it increases the reactivity of trifluoroethanol more than that of water.[24] The different behavior can be explained by an increase in the activity coefficient of trifluoroethanol relative to that of water as the [HOH]/[ROH] ratio is increased,[28] as well as a significant role for water as a hydrogen bond acceptor for the reaction of trifluoroethanol.[24]

Discussion

The Dependence of log *k* on the Structure of ROH and B. The Brønsted-type correlations of Figure 5A show that for the "uncatalyzed" (i.e., water catalyzed) reactions there is a larger dependence of log *k* on the basicity of the alcohol with Me_2N-R^+ than with the more reactive MeO–R^+ carbocation, in agreement with previous results.[25] However, for the acetate-catalyzed reaction, the dependence on alcohol structure is much smaller and the Me_2N-R^+ ion does not show a larger selectivity than MeO–R^+. The results are plotted against the pK_a of the conjugate acid of the primary amine that corresponds to the alcohol, pK_N, rather than the pK_a of the alcohol itself. The pK_N values give slightly better correlations, presumably because positive rather than negative charge is developed on the alcohol in the transition state for nucleophilic attack.[25] The slopes of the lines are $\beta_{nuc} = 0.36$ ($r = 0.991$) and 0.26 ($r = 0.981$) for the uncatalyzed reactions and 0.04 ($r = 0.494$) and 0.10 ($r = 0.810$) for the acetate-catalyzed reactions with Me_2N-R^+ and MeO–R^+, respectively. The equilibrium constant for alcohol addition is favored by electron-donating substituents in the alcohol, with $\beta_{eq} \sim 0.2$,[29] so that in the reverse reaction catalyzed by acetic acid there is a small development of negative charge on the alcohol, with $\beta_{lg} \sim 0.1 - 0.2 = -0.1$.

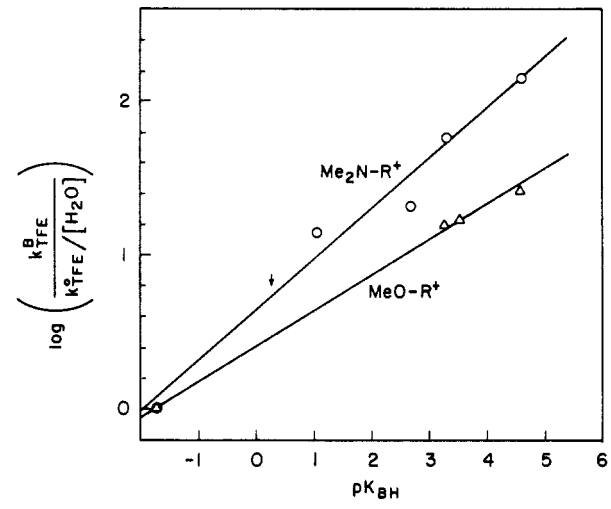

Figure 6. Brønsted plots for general base catalysis of the reaction of trifluoroethanol with 1-(4-(dimethylamino)phenyl)ethyl carbocation in 50:50 (v:v) H_2O:TFE and 1-(4-methoxyphenyl)ethyl carbocation in 50:45:5 (v:v:v) H_2O:TFE:MeOH.

It is apparent that the base-catalyzed reactions of trifluoroethanol and other weakly basic alcohols are more important for the Me_2N-R^+ cation. However, catalysis becomes relatively much less important for the more basic alcohols and is not detectable for methoxyethanol and ethanol.

A somewhat better correlation is obtained with use of the ratios k^0_{ROH}/k^0_{TFE} and k^B_{ROH}/k^B_{TFE} for the uncatalyzed and catalyzed reactions, respectively, as shown in Figure 5B. The improvement may be attributed to a small but significant solvent effect on k_{HOH} when 10% trifluoroethanol is replaced by 10% ROH in order to measure rate constants for the different alcohols, as described in the Results section. This solvent effect is smaller for k_{TFE} (Table V). The slopes in Figure 5B are $\beta_{nuc} = 0.39$ ($r = 0.997$) and 0.24 ($r = 0.989$) for the uncatalyzed reactions and 0.11 ($r = 0.965$) and 0.12 ($r = 0.914$) for the acetate-catalyzed reactions with Me_2N-R^+ and MeO–R^+, respectively. The experimental data reported here agree closely with those obtained previously; however, the values of β_{nuc} differ from the previously reported values of $\beta_{nuc} = 0.5$ and 0.32 for the uncatalyzed reactions of Me_2N-R^+ and MeO–R^+, respectively, because the earlier data were plotted against the pK_a of the alcohol and involved several different alcohols.[25]

The rate constants for general base catalysis of the addition of trifluoroethanol to Me_2N-R^+ follow a Brønsted correlation with a slope of $\beta = 0.33$ ($r = 0.998$), as shown in Figure 6. This is larger than the value of $\beta = 0.23$ ($r = 0.999$) for catalysis of

(26) Fife, T. H.; Anderson, E. *J. Am. Chem. Soc.* **1970**, *92*, 5464–5468. Fife, T. H.; Przystas, T. J. *J. Am. Chem. Soc.* **1980**, *102*, 292–299. Fife, T. H. *Acc. Chem. Res.* **1972**, *5*, 264–272. Jensen, J. L.; Jencks, W. P. *J. Am. Chem. Soc.* **1979**, *101*, 1476–1488.

(27) Kaspi, J.; Rappoport, Z. *J. Am. Chem. Soc.* **1980**, *102*, 3829–3837 and references therein.

(28) Water–trifluoroethanol mixtures show positive deviations from Raoult's law: Smith, L. S.; Tucker, E. E.; Christian, S. D. *J. Phys. Chem.* **1981**, *85*, 1120–1126.

(29) Rothenberg, M. E.; Richard, J. P.; Jencks, W. P. *J. Am. Chem. Soc.* **1985**, *107*, 1340–1346.

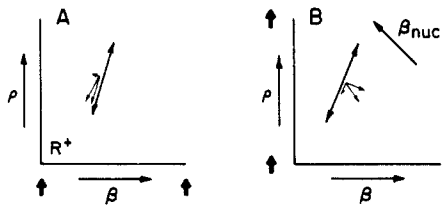

Figure 7. Enlargements of the region around reaction coordinate B in Figure 1 to show how the position of the transition state changes with destabilization of the carbocation (A) and increased basicity of the catalyst (B). The short heavy arrows represent an increase in σ that increases the energy at the bottom (A) and an increase in pK_B that increases the energy on the left side (B) of the diagram. The short arrows on the reaction coordinates represent movement of the transition state perpendicular and parallel to the direction of the reaction coordinate.

trifluoroethanol addition to MeO–R^+ (Figure 6). The catalytic constants are divided by the rate constants for the water-catalyzed reaction, to permit comparison of the results for the two carbocations on the same graph. The catalytic constants for both reactions were obtained by comparison with k_{HOH}, rather than k_{az},[11] as described in the Results section. The third-order rate constants for the water-catalyzed reactions of trifluoroethanol with both carbocations are consistent with the same correlation lines as the rate constants for substituted acetate anions.

The Dependence of β and β_{nuc} on the Structure of ROH, $ArEt^+$, and B. The decrease in β_{nuc} for the water-catalyzed attack of alcohols on MeO–R^+ compared with Me_2N–R^+ (Figure 5) means that polar substituents on the alcohol "see" less development of positive charge on the oxygen atom in the transition state for addition to MeO–R^+ compared with Me_2N–R^+. This is a normal "Hammond effect", with less bond formation to oxygen in the transition state when the electrophile is more reactive; MeO–R^+ is $\sim 10^5$ more reactive than Me_2N–R^+. It can be described by a positive value of the cross-interaction coefficient $p_{yy'} = \partial\beta_{nuc}/-\partial\sigma = \partial\rho/-\partial pK_{nuc} = 0.1$.[25] The $p_{yy'}$ coefficient describes changes in structure–reactivity behavior involving ROH and the carbocation.[17,20]

These structure–reactivity coefficients and changes in structure–reactivity coefficients may be described by the energy contour diagram of Figure 1. The coordinates of the diagram are defined by the observed, β, β_{nuc}, and ρ values, and the energy may be shown by contour lines, which are only indicated around the saddle points in Figure 1. Changes in structure–reactivity coefficients represent movements of the transition state parallel and perpendicular to the reaction coordinate that are determined by the direction of the reaction coordinate and the curvatures of the surface parallel and perpendicular to the reaction coordinate on the diagram.[20,21] The data for catalysis of the addition of ROH to Me_2N–R^+ and MeO–R^+ are consistent with reaction coordinate B in Figure 1, which is shifted slightly clockwise from the vertical.

The larger σ value for MeO–R^+ compared with Me_2N–R^+ represents a destabilization of the MeO–R^+ compared with the Me_2N–R^+ carbocation, so that the energy of the bottom of the diagram is higher for MeO–R^+ than for Me_2N–R^+. This can give a normal Hammond effect for the addition of ROH if the reaction coordinate is predominantly vertical, as shown in Figure 7A. The heavy arrows at the bottom of the diagram indicate the increase in energy of the carbocation. The transition state will tend to move toward the position of higher energy at the bottom of the diagram, parallel to the reaction coordinate, with a decrease in β_{nuc} and a positive value of $p_{yy'} = \partial\beta_{nuc}/-\partial\sigma$.[11]

The predominantly vertical reaction coordinate involves primarily nucleophilic attack of the alcohol on the carbocation and suggests that there is not a large amount of proton transfer from the attacking alcohol in the transition state. Proton removal would be expected to decrease the amount of positive charge development on the attacking oxygen atom and β_{nuc}. However, the hydroxyl group will certainly be hydrogen bonded to solvent molecules in the transition state, and added buffer bases might be expected to catalyze the reaction by hydrogen bonding to the hydroxyl group.[11]

The movement of the transition state downward and to the left in Figure 7A also corresponds to a decrease in β for general base catalysis. This is observed; the Brønsted values decrease from $\beta = 0.33$ for Me_2N–R^+ to $\beta = 0.23$ for MeO–R^+. The change in β is described by the cross-interaction coefficient p_{xy} (eq 4),

$$p_{xy} = \frac{\partial\beta}{-\partial\sigma} = \frac{\partial\rho}{-\partial pK_{BH}} \quad (4)$$

which describes changes in structure–reactivity behavior involving the base and the carbocation, at the two ends of the transition state. The decrease in β is consistent with significant diagonal character to the reaction coordinate; a completely vertical reaction coordinate would not be expected to give movement of the transition state to the left when the energy of the cation at the bottom of the diagram is increased.

Increasing the basicity of B raises the energy of the left compared with the right side of Figure 1, as shown by the heavy arrows in Figure 7B. This will tend to shift the transition state downhill, perpendicular to the reaction coordinate, toward the position of lower energy on the right side of Figure 7B. This corresponds to a decrease in charge development on the oxygen atom in the transition state and β_{nuc}. Figure 5 shows that there is a large decrease in β_{nuc} for the acetate-catalyzed compared with the water-catalyzed reactions.

The change in β_{nuc} is described by a positive $p_{xy'}$ coefficient (eq 5), which describes changes in structure–reactivity behavior involving the base and the attacking alcohol in the transition state. The same $p_{xy'}$ coefficient describes the increase in β with decreasing

$$p_{xy'} = \frac{\partial\beta}{-\partial pK_{nuc}} = \frac{\partial\beta_{nuc}}{-\partial pK_{BH}} \quad (5)$$

alcohol pK_a that makes general base catalysis detectable with weakly basic alcohols.

Changes in Interaction Coefficients and the Nature of the Transition State. Interaction coefficients describe changes in structure–reactivity parameters that define the energy surface in the immediate vicinity of the transition state and the movements of the saddle point when the energy of a side or corner of the diagram is changed.[20,21] Small or moderate changes in the nature of the transition state may be described by a particular value of an interaction coefficient. However, when changes in the parameters and movements of the transition state are large, the nature of the energy surface around the transition state will change. This *must* occur when the edge of the diagram is approached and the structure–reactivity parameters approach limiting values. These changes will give different interaction coefficients that reflect changes in the nature of the reaction coordinate and transition state. Eventually they will lead to a different reaction mechanism.

Figure 5 shows that β_{nuc} for the water-catalyzed addition of alcohols decreases with increasing σ for substituents on the carbocation, which corresponds to the positive $p_{yy'}$ coefficient that was described above. However, there is no such decrease for the acetate-catalyzed reaction. This means that $p_{yy'}$ decreases to a value close or equal to zero for the stronger base. The change in the $p_{yy'}$ interaction coefficient means that there is a change in the nature of the transition state as the catalyzing base becomes stronger. This change can be described by a positive $p^*_{xyy'}$ coefficient, as defined in eq 6. The first term in the $p^*_{xyy'}$ coefficient describes a change in the $p_{yy'}$ coefficient with changing pK_a of the base catalyst.

$$p^*_{xyy'} = \frac{\partial p_{yy'}}{-\partial pK_{BH}} = \frac{\partial p_{xy'}}{-\partial\sigma} = \frac{\partial p_{xy}}{-\partial pK_N} \quad (6)$$

These changes are illustrated more clearly by Figure 8. Figure 8A shows the dependence on pK_N of the logarithms of the ratios of the rate constants for reactions of alcohols with MeO–R^+ and Me_2N–R^+, "$\Delta\rho$" (eq 7).

$$\text{"}\Delta\rho\text{"} = \log \frac{(k_{ROH}/k_{HOH})_{MeO}}{(k_{ROH}/k_{HOH})_{Me_2N}} = \Delta\sigma(\rho_{ROH} - \rho_{HOH}) \quad (7)$$

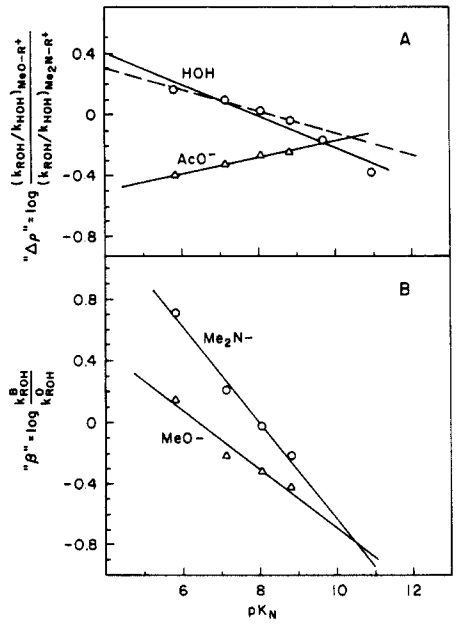

Figure 8. A: Plots of the rate constant ratios for the two 1-arylethyl carbocations ("ρ") against the nucleophilicity of the alcohol (pK_N) for the water-catalyzed and the acetate-catalyzed reactions. B: Plots of the ratios of the rate constants for the acetate- and water-catalyzed reactions ("β") against the nucleophilicity of the alcohol (pK_N) for the Me_2N–R^+ and the MeO–R^+ carbocations.

This ratio decreases with increasing pK of ROH for the water-catalyzed reaction but increases with increasing pK of ROH for the acetate-catalyzed reaction. The negative slope of −0.103 represents a positive value of $p_{yy'} = \partial\rho/-\partial pK_N$ while the positive slope of 0.053 represents a negative value of $p_{yy'}$. These changes correspond to a positive value of $p^*_{xyy'} = \partial p_{yy'}/-\partial pK_{BH}$.

Figure 8B shows another form of presenting the experimental data. With increasing pK of ROH the value of "β" = log (k^B_{ROH}/k^0_{ROH}), the logarithm of the ratio of the rate constants for the acetate-catalyzed and water-catalyzed reactions, decreases more steeply for the reaction with Me_2N–R^+ than with MeO–R^+. The negative slopes of −0.31 and −0.19 for Me_2N–R^+ and MeO–R^+, respectively, represent positive values of $p_{xy'}$. The change in slopes corresponds to a positive value of $p^*_{xyy'} = \partial p_{xy'}/-\partial\sigma$ (eq 6).

The lines in Figure 8A intersect at the point that the ratios of rate constants are equal according to eq 8, which can be transformed into eq 9. Equation 9 is the same as eq 10, which gives

$$\log \frac{(k^0_{ROH}/k_{HOH})_{MeO}}{(k^0_{ROH}/k_{HOH})_{Me_2N}} = \log \frac{(k^B_{HOH}/k_{HOH})_{MeO}}{(k^B_{ROH}/k_{HOH})_{Me_2N}} \quad (8)$$

the intersection point for the lines of Figure 8B; i.e., the lines of parts A and B of Figure 8 should intersect at the same point. Both

$$\log \frac{(k^B_{ROH}/k_{HOH})_{Me_2N}}{(k^0_{ROH}/k_{HOH})_{Me_2N}} = \log \frac{(k^B_{ROH}/k_{HOH})_{MeO}}{(k^0_{ROH}/k_{HOH})_{MeO}} \quad (9)$$

$$\log \left(\frac{k^B_{ROH}}{k^0_{ROH}}\right)_{Me_2N} = \log \left(\frac{k^B_{ROH}}{k^0_{ROH}}\right)_{MeO} \quad (10)$$

pairs of lines do intersect near $pK_N = 10$. The intersection point is $pK_N = 10.4$ if the upper line in Figure 8A is drawn only through the first four points (dashed line), as was done for the other three lines. For an alcohol of $pK_N = 10.4$, which corresponds to $pK_{ROH} = 15.4$, the value of β should be the same for reactions with all 1-phenylethyl carbocations. In other words, ρ becomes independent of the basicity of the catalyst and $p_{xy} = \partial\rho/-\partial pK_{BH} = 0$.

Figure 9 shows that the slopes of the plots of "$\Delta\rho$" against the pK_a of the base catalyst are negative and that the order of the points for the different alcohols is reversed for the two catalysts.

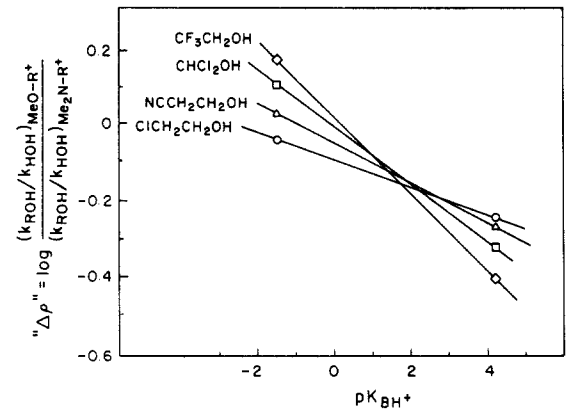

Figure 9. Plots of the rate constant ratios for the two 1-arylethyl carbocations ("ρ") against pK_{BH^+} of the two catalyzing bases for a series of substituted ethanols.

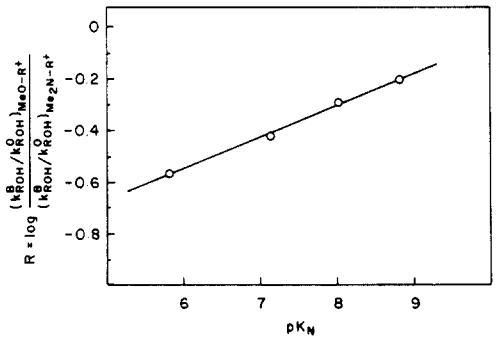

Figure 10. A plot to calculate the value of the interaction coefficient $p^*_{xyy'}$.

The negative slopes correspond to a positive value of $p_{xy} = \partial\rho/-\partial pK_{BH}$. The increasingly negative slopes with decreasing pK of the alcohol correspond to increasingly positive values of p_{xy} and a positive value of the coefficient $p^*_{xyy'} = \partial p_{xy}/-\partial pK_N$ (eq 6).

The value of $p^*_{xyy'}$ can be obtained directly from the experimental data by plotting the ratio $R = \log [(k^B_{ROH}/k^0_{ROH})_{MeO}/(k^B_{ROH}/k^0_{ROH})_{Me_2N}]$ against pK_N, which minimizes the effects of scatter in the individual plots. Such a plot is shown in Figure 10 and has a slope of 0.12 ($r = 0.998$). This slope is given by eq 11, which is obtained from eq 12. The value of ΔpK_{BH} is 4.6 − (−1.74) = 6.34 and a value of $\Delta\sigma = 1.75$ is obtained from the σ^n and

$$\frac{\partial R}{\partial pK_N} = \frac{-\partial p_{xy}}{\partial pK_N}\Delta\sigma\Delta pK_{BH} = p^*_{xyy'}\,\Delta\sigma\Delta pK_{BH} \quad (11)$$

σ^+ values for the two substituents and $r^+ = 2.1$, for a correlation of the reactivities of 1-phenylethyl carbocations with trifluoroethanol according to Yukawa and Tsuno (eq 13).[24,30] This gives a value of $p^*_{xyy'} = 0.011$.

$$R = \log \frac{(k^B_{ROH}/k^0_{ROH})_{MeO}}{(k^B_{ROH}/k^0_{ROH})_{Me_2N}} = (\beta_{MeO} - \beta_{Me_2N})\Delta pK_{BH} = \frac{\partial\beta}{\partial\sigma}(\sigma_{MeO} - \sigma_{Me_2N})\Delta pK_{BH} = -p_{xy}\Delta\sigma\Delta pK_{BH} \quad (12)$$

$$\log \left(\frac{k}{k_0}\right) = \sigma^n + r^+(\sigma^+ - \sigma^n) \quad (13)$$

The value of $p^*_{xyy'}$ can also be calculated from the correlations in Figure 8. The slope of each line in Figure 8A is $(\partial\rho_{ROH}/\partial pK_N)\Delta\sigma = -p_{yy'}\Delta\sigma$. The slopes of −0.103 and 0.053 give values of $p_{yy'} = 0.059$ and −0.030 for the water-catalyzed and acetate-catalyzed reactions, respectively. These values of $p_{yy'}$ give $p^*_{xyy'} = \partial p_{yy'}/\partial pK_{BH} = 0.014$. The same calculation with the dashed line through the first four points in Figure 8A gives $p^*_{xyy'} = 0.010$.

The slope of each line in Figure 8B is $(\partial\beta/\partial pK_N)\Delta pK_{BH} = -p_{xy'}\Delta pK_{BH}$. The slopes of −0.31 and −0.19 give values of $p_{xy'} = 0.049$ and 0.030 for the reactions with Me_2N–R^+ and MeO–R^+,

respectively. These values of $p_{xy'}$ give $p^*_{xyy'} = \partial p_{xy'}/-\partial\sigma = 0.011$.

Several points should be kept in mind if it is desired to make quantitative comparisons of these coefficients in different systems:

(1) The values of the interaction coefficients that are reported here are based on the observed structure–reactivity parameters. For comparison with other reactions, which may have a different ρ value for the equilibrium constants of the addition reaction, for example, they should be normalized to a common scale by using the structure–reactivity coefficients of the equilibrium reactions.[20]

(2) The absolute values of the $p_{yy'}$ coefficients are larger than the observed values because of an electrostatic interaction between the substituents on the alcohol and the electrophile that is independent of transition-state structure. The electrostatic interaction may be described by $\tau = \partial\beta_{eq}/\partial\sigma = \partial\rho_{eq}/\partial pK_{ROH} = 0.10$ for 1-arylethyl ethers.[29] However, this electrostatic correction does not influence the changes in $p_{yy'}$ that are considered here.

(3) There are several relationships between different interaction coefficients that are followed if the structure–reactivity coefficients of a reaction are "balanced", i.e., if changes in certain structure–reactivity coefficients are additive.[17] If the structure–reactivity coefficients are not balanced these relationships are not followed and changes in interaction coefficients will also not follow the corresponding additivity relationships.

Changes in the Nature of Transition States—Third Derivative Interaction Coefficients. Changes in rate constants with changing reactant structure are described by first derivatives of log k, such as β, β_{nuc}, and ρ. Changes in β, β_{nuc}, and ρ reflect changes in transition-state structure and are described by second derivatives of log k, such as the interaction coefficients p_x, p_{xy}, and $p_{yy'}$. Changes in the interaction coefficients are third derivatives of log k and represent changes in the *nature* of the transition state, i.e., changes of the direction of the reaction coordinate and curvatures of the surface, such as A, B, and C in Figure 1.

These changes must exist for most or all reactions because the nature of the energy surface that describes the reaction will change with sufficiently large changes in reactant structure. The approximation that the behavior of the transition state can be described by constant curvatures through a saddle point is reasonable for small changes but will fail for large changes in structure. In particular, there must be changes in the nature of the surface when the transition state approaches an edge of the diagram, where bond orders and structure–reactivity coefficients approach limiting values. It is probable that such changes also occur when changes in transition-state structure in the central region of the diagram are large because the approximation that the surface around the transition state is quadratic, while reasonable for small changes, is likely to fail for large changes in transition-state structure. These changes are of interest because they describe one way in which a change from one to another reaction mechanism can take place.

Olefin-forming elimination reactions also undergo major changes in transition-state structure that change the nature of the transition state with changing substituents. For example, the base-catalyzed elimination of 2-arylethyl halides proceeds through a fully concerted, coupled mechanism with a diagonal reaction coordination on an energy contour diagram. Electron-withdrawing substituents on the aryl group and poorer leaving groups cause a shift in the position of the transition state toward the carbanion in the upper left corner and also cause a shift to a more horizontal reaction coordinate near the top of the diagram.[31,32] One consequence of this is a change in direction of the change in β with increasing σ: electron-withdrawing groups on the benzene ring first cause an increase in β, from movement of the transition state perpendicular to the reaction coordinate, but then cause a decrease in β from movement of the transition state parallel to the reaction coordinate (a "Hammond effect") as the reaction coordinate becomes horizontal and proton transfer becomes the major component of the transition state.[32] This change in direction can also

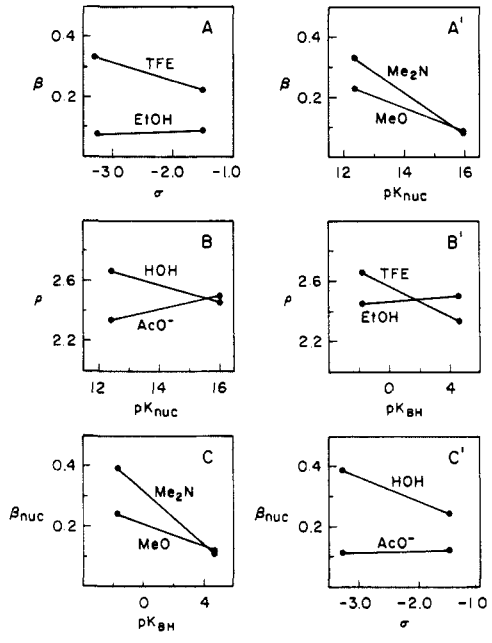

Figure 11. The interrelated changes in structure–reactivity coefficients that are described by the third derivative $p^*_{xyy'}$. Changes in β, β_{nuc}, and ρ are shown for different alcohols, carbocations, and catalysts as substituents are added to each reactant.

be regarded as an edge effect because the reaction coordinate can no longer be diagonal when it approaches the upper edge of the diagram, with $\beta_{lg} \sim 0$. Eventually, the reaction changes to an ElcB mechanism when the carbanion becomes stable enough to have a significant lifetime.[31-33]

It may not be immediately obvious how different changes in transition-state structure, such as those described here, are related to one another. It is well-known that general acid catalysis of ROH expulsion tends to disappear as ROH becomes less acidic and the electrophilic reagent becomes less stable, and that general base catalysis disappears as β approaches zero.[2-12] The relationships between these and other changes in structure–reactivity interaction coefficients are described by the third-derivative coefficients for class n reactions shown in Table VII. The table also includes coordinates for energy contour diagrams with x, y, and y' for β, ρ, and β_{nuc}, and d, e, and e' for $-pK_{BH}$, $-\sigma$, and $-pK_{nuc}$, respectively. Third-derivative coefficients for class e catalysis and for substitution reactions are also given in Table VII.

The way in which some of these interrelated changes in the nature of the transition state take place as the reaction coordinate approaches the left edge of the diagram in Figure 1 may be described as follows. They may also be described in several alternative sequences.

Class n reactions characteristically show a decrease in β (and an increase in α in the reverse direction) as the electrophilic reagent becomes less stable, which are described by a positive coefficient $p_{xy} = \partial\beta/-\partial\sigma = \partial\rho/-\partial pK_{BH}$. However, β cannot decrease below 0 (α cannot increase above 1.0) so that p_{xy} must also decrease and approach zero as σ increases, β decreases, and the reaction coordinate approaches the left edge of the diagram (Figure 1). This corresponds to a positive p^*_{xyy} coefficient (Table VII) and to the disappearance of general base catalysis. We might say that the positive p_{xy} coefficient carries within it the seeds of its own destruction.

The characteristic decrease in β with increasing pK_{nuc} for class n reactions is described by a positive coefficient $p_{xy'} = \partial\beta/-\partial pK_{nuc} = \partial\beta_{nuc}/-\partial pK_{BH}$. When β is small it will again approach the limit of zero so that $p_{xy'}$ will also decrease with increasing pK_{nuc} and the $p_{xy'y'}$ coefficient will be positive (Table VII).

The interrelated changes that are described by the $p^*_{xyy'}$ coefficient (eq 6, Table VII) are illustrated in Figure 11. The

(30) Yukawa, Y.; Tsuno, Y.; Sawada, M. *Bull. Chem. Soc. Jpn.* **1966**, *39*, 2274–2286. Hine, J. S. *Structural Effects on Equilibria in Organic Chemistry*; Wiley: New York, 1975; pp 55–78.
(31) Gandler, J.; Jencks, W. P. *J. Am. Chem. Soc.* **1982**, *104*, 1937–1951.
(32) Gandler, J. R.; Yokoyama, T. *J. Am. Chem. Soc.* **1984**, *106*, 130–135.
(33) Keefe, J. R.; Jencks, W. P. *J. Am. Chem. Soc.* **1983**, *105*, 265–279.

Table VII. Changes in Interaction Coefficients for Class *n*, Class *e*, and Substitution Reactions[a]

Term	Class n		Class e		Substitution		Diagram
p^*_{xxx}	$=\frac{\partial p_x}{-\partial pK_{BH}}$	$=\frac{\partial^2\beta}{-\partial pK_{BH}(-\partial pK_{BH})}$	$=\frac{\partial p_x}{\partial pK_{HA}}=\frac{\partial^2\alpha}{\partial pK_{HA}\partial pK_{HA}}$		$=\frac{\partial p_x}{-\partial pK_{nuc}}$	$=\frac{\partial^2\beta_{nuc}}{-\partial pK_{nuc}(-\partial pK_{nuc})}$	$=\frac{\partial^2 x}{\partial d\partial d}$
p^*_{yyy}	$=\frac{\partial p_y}{-\partial\sigma}$	$=\frac{\partial^2\rho}{-\partial\sigma(-\partial\sigma)}$	$=\frac{\partial p_y}{-\partial pK_{nuc}}=\frac{\partial^2\beta_{nuc}}{-\partial pK_{nuc}(-\partial pK_{nuc})}$		$=\frac{\partial p_y}{\partial pK_{lg}}$	$=\frac{-\partial^2\beta_{lg}}{\partial pK_{lg}\partial pK_{lg}}$	$=\frac{\partial^2 y}{\partial e\partial e}$
$p^*_{y'y'y'}$	$=\frac{\partial p_{y'}}{-\partial pK_{nuc}}$	$=\frac{\partial^2\beta_{nuc}}{-\partial pK_{nuc}(-\partial pK_{nuc})}$	$=\frac{\partial p_{y'}}{-\partial\sigma}=\frac{\partial^2\rho}{-\partial\sigma-\partial\sigma}$		$=\frac{\partial p_{y'}}{\partial\sigma}$	$=\frac{-\partial^2\rho}{\partial\sigma\partial\sigma}$	$=\frac{\partial^2 y'}{\partial e'\partial e'}$
p^*_{xxy}	$=\frac{\partial p_x}{-\partial\sigma}=\frac{\partial p_{xy}}{-\partial pK_{BH}}=\frac{\partial^2\beta}{-\partial pK_{BH}(-\partial\sigma)}$		$=\frac{\partial p_x}{-\partial pK_{nuc}}=\frac{\partial p_{xy}}{\partial pK_{HA}}=\frac{\partial^2\alpha}{\partial pK_{HA}(-\partial pK_{nuc})}$		$=\frac{\partial p_x}{\partial pK_{lg}}=\frac{\partial p_{xy}}{-\partial pK_{nuc}}=\frac{\partial^2\beta_{nuc}}{-\partial pK_{nuc}\partial pK_{lg}}$		$=\frac{\partial^2 x}{\partial d\partial e}$
p^*_{xyy}	$=\frac{\partial p_y}{-\partial pK_{BH}}=\frac{\partial p_{xy}}{-\partial\sigma}=\frac{\partial^2\rho}{-\partial pK_{BH}(-\partial\sigma)}$		$=\frac{\partial p_y}{\partial pK_{HA}}=\frac{\partial p_{xy}}{-\partial pK_{nuc}}=\frac{\partial^2\beta_{nuc}}{\partial pK_{HA}(-\partial pK_{nuc})}$		$=\frac{\partial p_y}{-\partial pK_{nuc}}=\frac{\partial p_{xy}}{\partial pK_{lg}}=\frac{-\partial^2\beta_{lg}}{-\partial pK_{nuc}\partial pK_{lg}}$		$=\frac{\partial^2 y}{\partial d\partial e}$
$p^*_{xxy'}$	$=\frac{\partial p_x}{-\partial pK_{nuc}}=\frac{\partial p_{xy'}}{-\partial pK_{BH}}=\frac{\partial^2\beta}{-\partial pK_{BH}(-\partial pK_{nuc})}$		$=\frac{\partial p_x}{-\partial\sigma}=\frac{\partial p_{xy'}}{\partial pK_{HA}}=\frac{\partial^2\alpha}{\partial pK_{HA}(-\partial\sigma)}$		$=\frac{\partial p_x}{\partial\sigma}=\frac{\partial p_{xy'}}{-\partial pK_{nuc}}=\frac{\partial^2\beta_{nuc}}{-\partial pK_{nuc}\partial\sigma}$		$=\frac{\partial^2 x}{\partial d\partial e'}$
$p^*_{xy'y'}$	$=\frac{\partial p_{y'}}{-\partial pK_{BH}}=\frac{\partial p_{xy'}}{-\partial pK_{nuc}}=\frac{\partial^2\beta_{nuc}}{-\partial pK_{BH}(-\partial pK_{nuc})}$		$=\frac{\partial p_{y'}}{\partial pK_{HA}}=\frac{\partial p_{xy'}}{-\partial\sigma}=\frac{\partial^2\rho}{\partial pK_{HA}(-\partial\sigma)}$		$=\frac{\partial p_{y'}}{-\partial pK_{nuc}}=\frac{\partial p_{xy'}}{\partial\sigma}=\frac{-\partial^2\rho}{-\partial pK_{nuc}\partial\sigma}$		$=\frac{\partial^2 y'}{\partial d\partial e'}$
$p^*_{yyy'}$	$=\frac{\partial p_y}{-\partial pK_{nuc}}=\frac{\partial p_{yy'}}{-\partial\sigma}=\frac{\partial^2\rho}{-\partial\sigma(-\partial pK_{nuc})}$		$=\frac{\partial p_y}{-\partial\sigma}=\frac{\partial p_{yy'}}{-\partial pK_{nuc}}=\frac{\partial^2\beta_{nuc}}{-\partial pK_{nuc}(-\partial\sigma)}$		$=\frac{\partial p_y}{\partial\sigma}=\frac{\partial p_{yy'}}{\partial pK_{lg}}=\frac{-\partial\beta^2 lg}{\partial pK_{lg}\partial\sigma}$		$=\frac{\partial^2 y}{\partial e\partial e'}$
$p^*_{yy'y'}$	$=\frac{\partial p_{y'}}{-\partial\sigma}=\frac{\partial p_{yy'}}{-\partial pK_{nuc}}=\frac{\partial^2\beta_{nuc}}{-\partial\sigma(-\partial pK_{nuc})}$		$=\frac{\partial p_{y'}}{-\partial pK_{nuc}}=\frac{\partial p_{yy'}}{-\partial\sigma}=\frac{^2\rho}{-\partial pK_{nuc}(-\partial\sigma)}$		$=\frac{\partial p_{y'}}{\partial pK_{lg}}=\frac{\partial p_{yy'}}{\partial\sigma}=\frac{-\partial^2\rho}{\partial pK_{lg}\partial\sigma}$		$=\frac{\partial^2 y'}{\partial e\partial e'}$
$p^*_{xyy'}$	$=\frac{\partial p_{xy}}{-\partial pK_{nuc}}=\frac{\partial^2\beta}{-\partial\sigma(-\partial pK_{nuc})}$		$=\frac{\partial p_{xy}}{-\partial\sigma}=\frac{\partial^2\alpha}{-\partial pK_{nuc}(-\partial\sigma)}$		$=\frac{\partial p_{xy}}{\partial\sigma}=\frac{-\partial^2\beta_{nuc}}{\partial pK_{lg}\partial\sigma}$		$=\frac{\partial^2 x}{\partial e\partial e'}$
$p^*_{xyy'}$	$=\frac{\partial p_{yy'}}{-\partial pK_{BH}}=\frac{\partial^2\rho}{-\partial pK_{BH}(-\partial pK_{nuc})}$		$=\frac{\partial p_{yy'}}{\partial pK_{HA}}=\frac{\partial^2\beta_{nuc}}{\partial pK_{HA}(-\partial\sigma)}$		$=\frac{\partial yy'}{-\partial pK_{nuc}}=\frac{-\partial^2\beta_{lg}}{-\partial pK_{nuc}\partial\sigma}$		$=\frac{\partial^2 y}{\partial d\partial e'}$
$p^*_{xyy'}$	$=\frac{\partial p_{xy'}}{-\partial\sigma}=\frac{\partial^2\beta_{nuc}}{-\partial pK_{BH}(-\partial\sigma)}$		$=\frac{\partial p_{xy'}}{-\partial pK_{nuc}}=\frac{\partial^2\rho}{\partial pK_{HA}(-\partial pK_{nuc})}$		$=\frac{\partial_{xy'}}{\partial pK_{lg}}=\frac{-\partial^2\rho}{-\partial pK_{nuc}\partial pK_{lg}}$		$=\frac{\partial^2 y'}{\partial d\partial e}$

[a] The terms and coordinates of the diagrams are defined in the text or in ref 17, 20, and 21.

values of β are smaller and change more slowly with σ for ethanol, compared with trifluoroethanol (Figure 11, part A). This corresponds to a smaller p_{xy} coefficient, $\partial\beta/-\partial\sigma$, for the more basic alcohol and to a positive $p_{xyy'}$ coefficient, $\partial p_{xy}/-\partial pK_{nuc}$. The same data plotted against pK_{nuc} (Figure 11, part A′) show that β decreases more slowly with increasing pK_{nuc} for MeO–R^+ than for Me_2N–R^+. This corresponds to a decrease in $p_{xy'} = \partial\beta/-\partial pK_{nuc}$ with increasing σ and to the same $p^*_{xyy'}$ coefficient, as shown in eq 14. The interrelated decreases in β with increasing σ and β_{nuc} reflect the decreasing importance of catalysis with unstable

$$p^*_{xyy'} = \frac{\partial^2\beta}{-\partial\sigma(-pK_{nuc})} = \frac{\partial p_{xy}}{-\partial pK_{nuc}} = \frac{\partial p_{xy'}}{-\partial\sigma} \qquad (14)$$

carbocations and basic alcohols, respectively. The smaller decreases of the lower lines reflect the change to a transition state with a larger vertical component and a smaller component of proton transfer, B in Figure 1.

The value of ρ increases more with decreasing pK_{nuc} for the water-catalyzed reaction than for the acetate-catalyzed reaction (Figure 11, part B). This corresponds to a larger $p_{yy'}$ coefficient, $\partial\rho/-\partial pK_{nuc}$, for the less basic catalyst and to a positive $p^*_{xyy'}$ coefficient, $\partial p_{yy'}/-\partial pK_{BH}$. It means that the water-catalyzed reaction of trifluoroethanol is more important for MeO–R^+ than for Me_2N–R^+ so that buffer catalysis is less important for addition to the MeO–R^+ cation. The same data plotted against pK_{BH} (Figure 11, part B′) show that ρ increases more with decreasing catalyst pK_a for trifluoroethanol than for the more basic ethanol. This corresponds to a larger increase in $p_{xy} = \partial\rho/-\partial pK_{BH}$ for trifluoroethanol compared with ethanol. These changes represent a second expression of the $p^*_{xyy'}$ coefficient, as shown in eq 15.

$$p^*_{xyy'} = \frac{\partial^2\rho}{-\partial pK_{BH}(-\partial pK_{nuc})} = \frac{\partial p_{xy}}{-\partial pK_{nuc}} = \frac{\partial p_{yy'}}{-\partial pK_{BH}} \qquad (15)$$

The larger increase in β_{nuc} with decreasing basicity of the catalyst for Me_2N-R^+, compared with $MeO-R^+$ (Figure 11, part C), corresponds to an increase in $p_{xy'} = \partial\beta_{nuc}/-\partial pK_{BH}$ with decreasing σ. It means that the water-catalyzed reaction of basic alcohols is more significant for the dimethylamino compound and overwhelms the acetate-catalyzed reaction (Figure 5). It follows directly that there is a larger increase in β_{nuc} with decreasing σ for the water compared with the acetate-catalyzed reaction (Figure 11, part C'). The small value of β_{nuc} for the acetate-catalyzed reaction with both carbocations makes catalysis detectable with weakly basic alcohols. This represents an increase in $p_{yy'} = \partial\beta_{nuc}/-\partial\sigma$ for the water-catalyzed compared with the acetate-catalyzed reaction. Both of these changes correspond to the third expression of the $p^*_{xyy'}$ coefficient, as shown in eq 16.

$$p^*_{xyy'} = \frac{\partial^2\beta_{nuc}}{-\partial\sigma(-\partial pK_{BH})} = \frac{\partial p_{xy'}}{-\partial\sigma} = \frac{\partial p_{yy'}}{-\partial pK_{BH}} \quad (16)$$

The common terms in eq 14-16 show that these three expressions of the $p^*_{xyy'}$ coefficient are equal to each other. In fact, all of the relationships in eq 14-16 can be obtained directly from eq 17.

$$\frac{\partial^3 \log k}{-\partial pK_{BH}(-\partial pK_{ROH})(-\partial\sigma)} \quad (17)$$

Conclusion. The third-derivative interaction coefficients described here provide a means of characterizing the interrelated changes in transition-state structure and structure-reactivity coefficients that occur as the nature of a reaction mechanism changes. These changes occur as the transition-state structure and structure-reactivity coefficients approach limiting values. They probably also occur for transition states of intermediate structure because the energy surfaces that describe these reactions and their structure-reactivity behavior are not likely to follow simple quadratic equations when changes in transition-state structure are large.

Registry No. 4,4'-$H_3COC_6H_4CH(CH_3)OCOC_6H_4NO_2$, 58287-11-9; 4-$(H_3C)_2NC_6H_4CH(CH_3)OCH_3$, 94670-10-7; 4-$H_3COC_6H_4CHCH_3^+$, 18207-33-5; 4-$(H_3C)_2NC_6H_4CHCH_3^+$, 82414-94-6; H_2O, 7732-18-5; CF_3CH_2OH, 75-89-8; Cl_2CHCH_2OH, 598-38-9; $NCCH_2CH_2OH$, 109-78-4; $ClCH_2CH_2OH$, 107-07-3; $H_3COCH_2CH_2OH$, 109-86-4; H_3CCH_2OH, 64-17-5; $HSCH_2CH_2CH_3$, 107-03-9; $H_3CCO_2^-$, 71-50-1; $H_3COCH_2CO_2^-$, 20758-58-1; $ClCH_2CO_2^-$, 14526-03-5; $Cl_2CHCO_2^-$, 13425-80-4; $CF_3CO_2^-$, 14477-72-6.

General Acid Catalyzed Acetal Hydrolysis. The Hydrolysis of Acetals and Ketals of *cis*- and *trans*-1,2-Cyclohexanediol. Changes in Rate-Determining Step and Mechanism as a Function of pH

Thomas H. Fife* and R. Natarajan[1]

Contribution from the Department of Biochemistry, University of Southern California, Los Angeles, California 90033. *Received January 21, 1986*

Abstract: The plots of log k_{obsd} vs. pH for the hydrolysis of *cis*- and *trans*-1,2-cyclohexanediol isopropylidene ketal in 50% dioxane-H_2O (v/v) at 30 °C are linear with slopes of -1.0. The second-order rate constant for hydronium ion catalysis k_H is five-fold larger with the trans derivative than the cis, which is very likely due to the increased steric strain in the trans configuration. The plot of log k_{obsd} vs. pH for hydrolysis of *cis*-1,2-cyclohexanediol *p*-(dimethylamino)benzylidene acetal in H_2O at 30 °C is pH independent from pH 1 to 4 and linear with a slope of -1.0 at pH >5, quite similar to the profiles of other acetals of *p*-(dimethylamino)benzaldehyde. However, the log k_{obsd}-pH profile for the corresponding trans acetal is quite complex and shows seven inflections on the pH scale (1-13) only one of which is due to an ionization (the pK_a of the *p*-dimethylamino group conjugate acid). The other six inflections are due to changes in mechanism or rate-determining step as the pH is changed. At pH 1-6 hydronium ion and water-catalyzed hydrolysis of the hemiacetal intermediate is rate determining. At pH >6 attack of H_2O on the oxocarbonium ion intermediate becomes rate limiting, and at pH >7.3 OH^- attack on the oxocarbonium ion occurs. At pH >8 the rate-determining step changes to hydronium ion catalyzed ring opening ($k_H = 1.0 \times 10^6$ M^{-1} s^{-1} at 30 °C). Ring opening is catalyzed by various general acids with $\alpha \sim 0.7$. The plots of k_{obsd} vs. buffer concentration are linear with the exception of those determined in carbonate buffer with which there is pronounced curvature due to a change in the rate-determining step with increasing carbonate buffer concentration. The limiting value of k_{obsd} at higher buffer concentration is that for attack of OH^- on the oxocarbonium ion. At pH >10 the formation of aldehyde is pH independent, which indicates a unimolecular or water-catalyzed decomposition of the acetal. Thus, in the remarkable log k_{obsd} vs. pH profile for hydrolysis of *trans*-1,2-cyclohexanediol *p*-(dimethylamino)benzylidene acetal *all* of the mechanisms and rate-determining steps for acetal hydrolysis are represented on one plot. This is because of steric strain and the cyclic structure of the acetal, i.e., ring opening is rapid but is nevertheless reversible so that each step becomes rate limiting in turn as pH is increased.

The hydronium ion catalyzed hydrolysis of cyclic acetals proceeds as in eq 1.[2-6] Thus, there are three possible rate-determining steps. Acyclic acetals hydrolyze in the same manner except that the alcohol leaving group in the initial reaction is expelled into the solvent so that reversibility is minimized. The breakdown of the protonated acetal to a resonance stabilized oxocarbonium ion is generally the rate-determining step in the hydrolysis of simple acetals.[7] General acid catalysis has been observed in the hydrolysis of phenolic acetals with which the leaving group is very good and the oxocarbonium ion is of moderate stability,[8,9] and also in the

(1) Post-doctoral fellow, University of Southern California.
(2) Fife, T. H.; Jao, L. K. *J. Org. Chem.* **1965**, *30*, 1492.
(3) Ceder, O. *Ark. Kemi* **1954**, *6*, 523.
(4) Salomaa, P.; Kankaanpera, A. *Acta Chem. Scand.* **1961**, *15*, 871. Salomaa, P. *Suomen Kemistil. B* **1964**, *B37*, 86.
(5) Fife, T. H.; Hagopian, L. *J. Org. Chem.* **1966**, *31*, 1772.
(6) Fife, T. H.; Natarajan, R. *J. Am. Chem. Soc.* **1986**, *108*, 2425.
(7) Fife, T. H. *Acc. Chem. Res.* **1972**, *5*, 264.
(8) Fife, T. H.; Brod, L. H. *J. Am. Chem. Soc.* **1970**, *92*, 1681. Fife, T. H.; Jao, L. K. *J. Am Chem. Soc.* **1968**, *90*, 4081.

0002-7863/86/1508-8050$01.50/0